AFRL-RD-PS-
TR-2009-1085

COMPUTATIONAL SIMULATION OF HIGH ENERGY DENSITY PLASMAS

Michael H. Frese
Sherry D. Frese

NumerEx
2309 Renard SE, Suite 220
Albuquerque, NM 87106

30 October 2009

Final Report

AIR FORCE RESEARCH LABORATORY
Directed Energy Directorate
3550 Aberdeen Ave SE
AIR FORCE MATERIEL COMMAND
KIRTLAND AIR FORCE BASE, NM 87117-5776

Using Government drawings, specifications, or other data included in this document for any purpose other than Government procurement does not in any way obligate the U.S. Government. The fact that the Government formulated or supplied the drawings, specifications, or other data does not license the holder or any other person or corporation; or convey any rights or permission to manufacture, use, or sell any patented invention that may relate to them.

This report was cleared for public release by the Air Force Research Laboratory Philips Research Site Public Affairs Office and is available to the general public, including foreign nationals. Copies may be obtained from the Defense Technical Information Center (DTIC) (http://www.dtic.mil).

AFRL-DE-PS-TR-2009-1085 HAS BEEN REVIEWED AND IS APPROVED FOR PUBLICATION IN ACCORDANCE WITH ASSIGNED DISTRIBUTION STATEMENT.

James H. Degnan

Dr James H. Degnan, DR-IV
Project Manager

Wallace T. Clark

Dr. Wallace T. Clark III, DR-IV
Chief, High Power Microwave Division

This report is published in the interest of scientific and technical information exchange, and it's publication does not constitute the Government's approval or disapproval of its ideas or finding

REPORT DOCUMENTATION PAGE

Form Approved
OMB No. 0704-0188

1. REPORT DATE *(DD-MM-YYYY*	2. REPORT TYPE	3. DATES COVERED *(From - To)*
30-10-2009	Final Report	16 Sep 2005 - 30 Sep 2009

4. TITLE AND SUBTITLE
Computational Simulation of High Energy Density Plasmas

5a. CONTRACT NUMBER
FA9451-05-D-0157/0002

5b. GRANT NUMBER

5c. PROGRAM ELEMENT NUMBER
69120F

6. AUTHOR(S)
Michael H. Frese, Sherry D. Frese

5d. PROJECT NUMBER
DOES

5e. TASK NUMBER
HB

5f. WORK UNIT NUMBER
AA

7. PERFORMING ORGANIZATION NAME(S) AND ADDRESS(ES)

NumerEx
2309 Renard Place SE, Suite 220
Albuquerque, NM 87106

8. PERFORMING ORGANIZATION REPORT NUMBER

09-04

9. SPONSORING / MONITORING AGENCY NAME(S) AND ADDRESS(ES)
Air Force Research Laboratory
3550 Aberdeen Ave SE
Kirtland AFB, NM 87117-5776

10. SPONSOR/MONITOR'S ACRONYM(S)
AFRL/RDHP

11. SPONSOR/MONITOR'S REPORT NUMBER(S)
AFRL-RD-PS-TR-2009-1085

12. DISTRIBUTION / AVAILABILITY STATEMENT
APROVED FOR PUBLIC RELEASE, DISTRIBUTION IS UNLIMITED

13. SUPPLEMENTARY NOTES
377ABW-2010-0367

14. ABSTRACT

Plasmas with embedded high magnetic fields are less subject to thermal conduction losses and can therefore reach higher temperatures under compression. This effect offers a path to generation of neutrons by thermal collisions known as magnetized target fusion (MTF), now also referred to as magneto-inertial fusion (MIF). Since MTF allows the use of slower drivers for compression, it should lower the cost of achieving intense neutron pulses. NumerEx's effort under this Task Order has focused on two different concepts for MTF. The first approach is the generation, stagnation, and compression of ultrahigh speed plasma (UHP) flow; the second is formation, translation, capture, and compression of a field-reversed magnetized plasma configuration (FRC). In both concepts, the ultimate compression is by an imploding liner driven by a fast capacitor bank Here we will describe our achievements in simulating those two concepts. The first section will focus on simulations of the UHP target liner compression, and the second, on simulations of FRC compression.

15. SUBJECT TERMS
Computational simulation, high energy density plasmas, intense neutron sources, ultrahigh speed plasma, field reversed configuration, magnetized target fusion

16. SECURITY CLASSIFICATION OF:			17. LIMITATION OF ABSTRACT	18. NUMBER OF PAGES	19a. NAME OF RESPONSIBLE PERSON
a. REPORT	b. ABSTRACT	c. THIS PAGE			Dr. James H. Degnan
Unclassified	Unclassified	Unclassified	SAR	22	19b. TELEPHONE NUMBER *(include area code)* 505-846-1235

Standard Form 298 (Rev. 8-98)
Prescribed by ANSI Std. 239.18

THIS PAGE INTENTIONALLY LEFT BLANK

CONTENTS

Section **Page**

FIGURES

1. Introduction

Plasmas with embedded high magnetic fields are less subject to thermal conduction losses and can therefore reach higher temperatures under compression. This effect offers a path to generation of neutrons by thermal collisions known as magnetized target fusion (MTF), now also referred to as magneto-inertial fusion (MIF). Since MTF allows the use of slower drivers for compression, it should lower the cost of achieving intense neutron pulses.

NumerEx's effort under this Task Order has focused on two different concepts for MTF. The first approach is the generation, stagnation, and compression of ultrahigh speed plasma (UHP) flow; the second is formation, translation, capture, and compression of a field-reversed magnetized plasma configuration (FRC). In both concepts, the ultimate compression is by an imploding liner driven by a fast capacitor bank

Here we will describe our achievements in simulating those two concepts. The first section will focus on simulations of the UHP target liner compression[1], and the second, on simulations of FRC compression[2].

[1] P.J. Turchi, N.F. Roderick, J.H. Degnan, M.H. Frese, and D.J. Amdahl, "Preparation and Liner Compression of Plasma From an Ultrahigh Speed Flow," IEEE Trans. Plas. Sc., V36, 1, February 2008, pg. 92-98.

[2] E.L. Ruden, S. Zhang, T.P. Intrator, and G.A. Wurden, "Experimental Profile Evolution of a High-Density Field-reversed Configuration," Phys. Plas., V 13, 2006, pg. 13.122505-1.

2. Ultrahigh Speed Plasma Compression

The strength of the UHP approach is it can be implemented with a single pulsed power driver to create the magnetized plasma target and implode the compression liner. In order to do that with the AFRL/RDH Shiva Star fast capacitor bank, the liner may need to be made of lithium, which can be made lighter than the aluminum liners previously imploded.

Below, we will first describe a simulation addressing the physics of an imploding lithium liner. Then we will describe a simulation of a single integrated UHP load showing formation, stagnation, and compression driven at Shiva Star current and voltage.

2.1 Lithium Liner Dynamics

As part of its DETAR efforts, NumerEx supported AFRL's concept design effort for a high energy density magnetized plasma source. The design effort studied a concept consisting of a plasma flow switch (PFS) combined with a liner implosion. This suite of simulations performed by NumerEx used a layered approach, building progressively more detailed simulations via the addition of component models and more complex physics.

NumerEx started the design effort by examining a set of liner simulations with various materials at multiple radii to determine the materials' temperature, density, and speed at pinch. Figure 1 shows the liner state versus the radius of a collapsing 10 cm tall lithium liner driven by an RLC circuit model of Shiva Star. This work progressed by adding the PFS to the imploding liner simulations. The PFS creates high temperature magnetized plasma that serves as the target for the imploding liner. The PFS depends on a lithium barrier foil slowing the advance of deuterium up the coaxial gun to the corner. There the plasma behind the foil expands rapidly into the implosion volume.

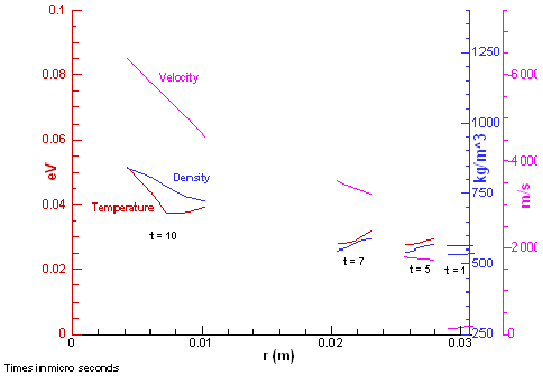

Figure 1 Liner Temperature, Density and Velocity versus Radius at Four Time Intervals.

2.1.1 Integrated UHP Load for Shiva Star

The configuration of the combined PFS and liner implosion is shown in Figure 2. The armature in the figure is the barrier foil. Initial simulations started at 5 μs with the barrier lithium foil and lithium liner moving and with current already flowing in the system. These

simulations illustrate the challenge of the integrated system: the difficulty separating the barrier foil from the plasma, the complexity of the MHD turning the plasma from the PFS to the implosion region, and the difficulty containing the plasma in the implosion region. Overall, these simulations provided the first insight into the plasma's physical properties, and showed the potential to meet the requirements of temperature and density.

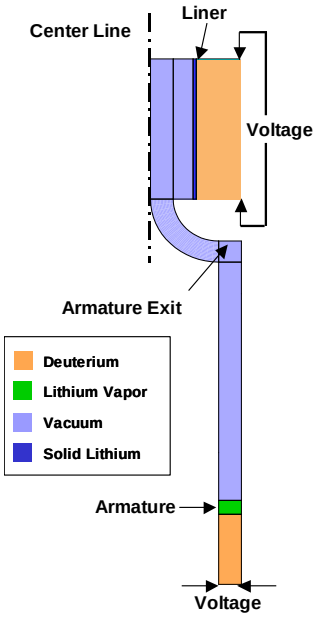

Figure 2 MACH2 Geometry of PFS Combined with Liner Implosion Region.

The next set of simulations started at time zero with a stationary barrier foil and liner, and no current flowing. These simulations produced new challenges of eroding the barrier foil due to the driving magnetic field, maintaining the proper current profile, ensuring proper timing between the plasma and liner implosion, and pinching a pure deuterium plasma. These simulations showed the plasma entering the liner implosion region at approximately 7 μs with pinch occurring at approximately 13 μs. Figure 3 shows the plasma turning the PFS corner in the coaxial gun section, and Figure 4 shows the physical state of the plasma just prior to pinch. Figure 5 shows neutron yield reaching 10^{14} in this simulation. These results have supported an AF Scientific Advisory Board review, APS poster sessions, and an IEEE publication.

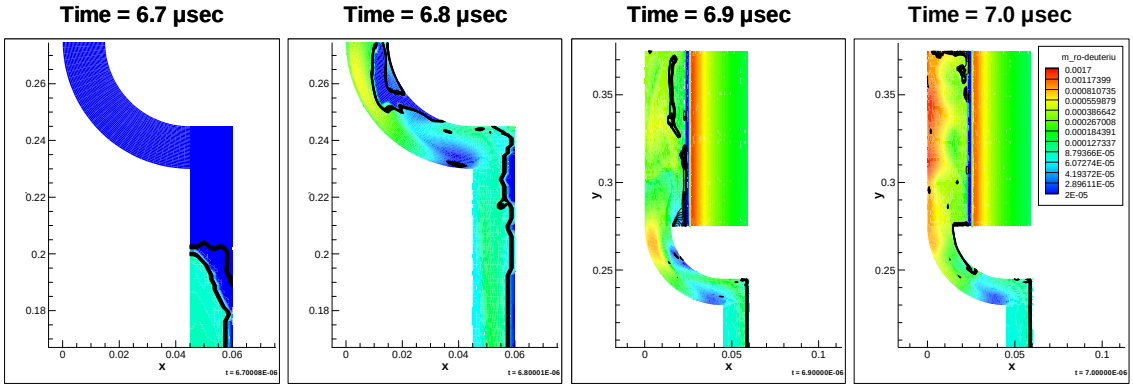

Figure 3 Magnetized Plasma Flowing Around Corner and Filling Liner Implosion Region.

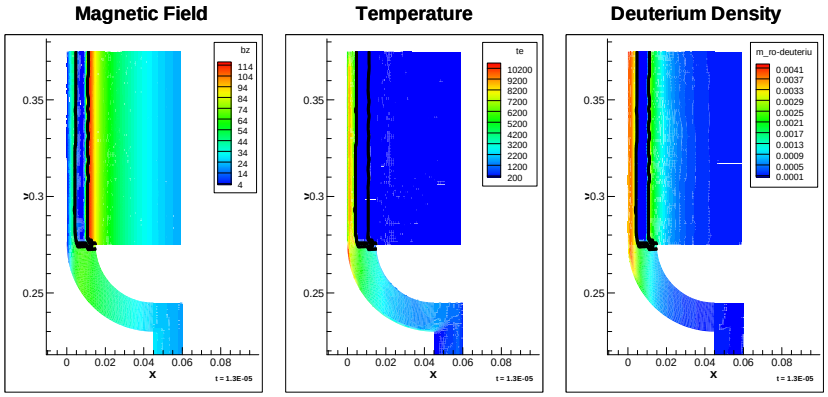

Figure 4 Magnetized Field, Temperature, and Density at 13 μs in Liner Implosion Region.

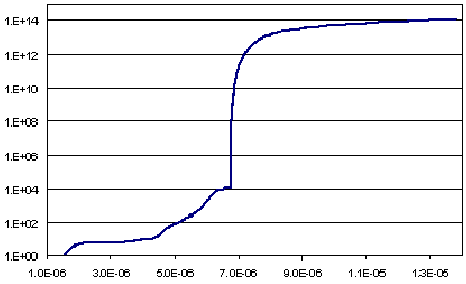

Figure 5 Neutron Yield vs. Time for Liner Implosion of a Magnetized Plasma.

Another set of simulations focused on injecting the deuterium into the PFS gun section. The injection technique needs to fill the region behind the barrier foil while minimizing the amount of deuterium gas traveling the opposite direction past the injection port. The left diagram in Figure 6 shows the full, axisymmetric MACH2 simulation geometry. Figure 6's second image details the channel geometry between the center cylinder and coaxial gas gun. The deuterium injection starts when the pressure of the deuterium gas in the bottom half of the center cylinder is released. A diaphragm keeps the deuterium in the center cylinder separate from the vacuum in PFS, and bursts quickly, allowing the deuterium gas to expand and accelerate to the top of the center cylinder. After hitting the top of the center cylinder, a shock forms and travels back down through the deuterium gas toward the radial ports. When the shock reaches the ports, the deuterium gas accelerates through the radial ports and exits vertically into the PFS. The channel width for the final vertical turn widens to help accelerate the supersonic flow. NumerEx used MACH2 to simulate the flow using compressible, inviscid hydrodynamics with the SESAME equations of state. The depth of the coaxial shock tube has been varied along with the initial density and pressure of the deuterium gas.

The work ahead requires interactively and iteratively designing a set of experiments, and performing the necessary post-experiment analysis. Some of the physics challenges remaining include full understanding of this deuterium injection into the PFS, the deuterium interaction

with the barrier foil and magnetic field, the motion of the plasma and barrier foil traveling through the PFS to the liner collapse, and the separation of the barrier foil from the plasma.

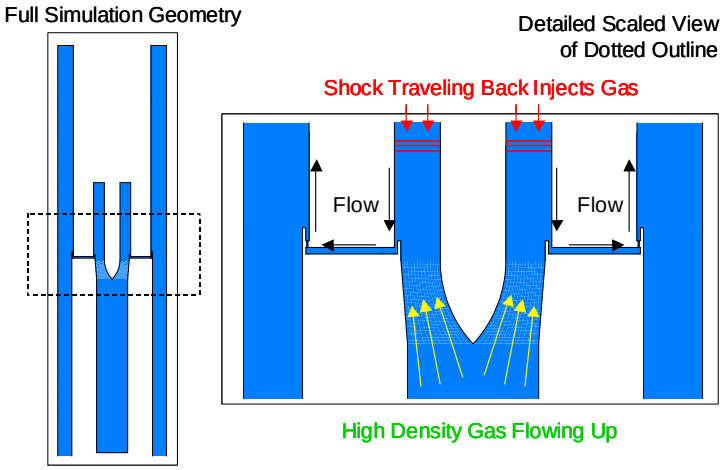

Figure 6 Geometry of the Gas Injection Hardware.

3. Field Reversed Configuration Compression

The strength of the FRC approach is that it produces a very controlled magnetized plasma target, at the expense of a relatively complex formation process driven by multiple pulsed power drivers. The first experiments addressed this formation process alone.

The experiments will then turn to formation of an FRC in a conical region, its subsequent translation out of that region and through a guide field to a magnetic mirror region where it will be captured, first inside a stationary mockliner, and later, a compressing liner.

Finally, there is the issue of development of rotation of the FRC. Such rotation can deform the FRC through a rotational instability, cause it to contact the wall, and destroy it.

Below we will first describe our recent integrated simulation of the formation, translation, capture, and compression of the FRC. These simulations, including only the usual advective and resistive terms of Ohm's Law do not produce rotation in the FRC. We will then describe extended magnetohydrodynamic (XMHD) simulations of the formation process which do show rotation in the context of an FRC formation experiment at AFRL/RDH.

3.1 Integrated Simulation of FRC Formation, Translation, Capture, and Compression

Over the past two years, NumerEx has made great strides in increasing the fidelity of its fully integrated FRC formation, translation, and compression simulations using MACH2. We have also improved our ability to modify detail of our simulations quickly, making us more responsive to changes in the experiment's design.

More recently, we have updated our simulations to the actual dimensions and field strengths of the planned experiments. These simulations require greater accuracy because of the smaller fields and larger experiment. Hence we have improved several algorithms used in the simulations and applied MACH2's adaptive mesh capabilities to the FRC. We have also extended the diagnostics produced by MACH2.

In conjunction with AFRL experimentalists and theoreticians, we have been able to use these simulations to explore suggestions for design improvements and experimental parameters. The following shows a specific example of how these simulations have been used.

Figure 7 shows our typical 2D MTF simulation setup. The axis of symmetry is at the bottom of the figure. The FRC is formed on the right hand side, while the liner, on the left, is being imploded[3].

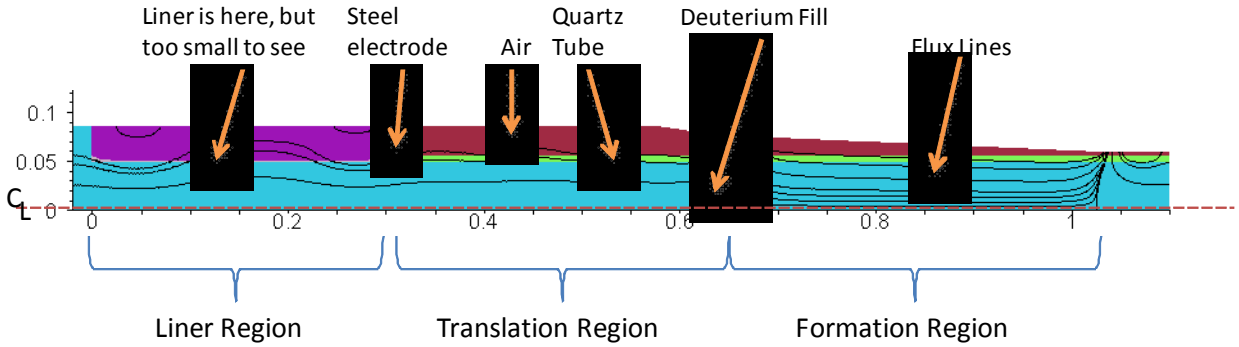

Figure 7 Diagram of the materials and scale of the 2D simulations. The flux lines shown are from the initial bias field.

Typically, the liner implosion is started prior to the firing of the main bank for FRC formation. Figure 8 shows a typical simulation in which the FRC formation began 5.2 μs after the firing of Shiva Star. Within 4 μs the FRC is poised to enter the liner.

The relative strengths of the various fields, the angle of the formation cone, and the timing of the FRC formation relative to the implosion of the liner are all important to the eventual capture and

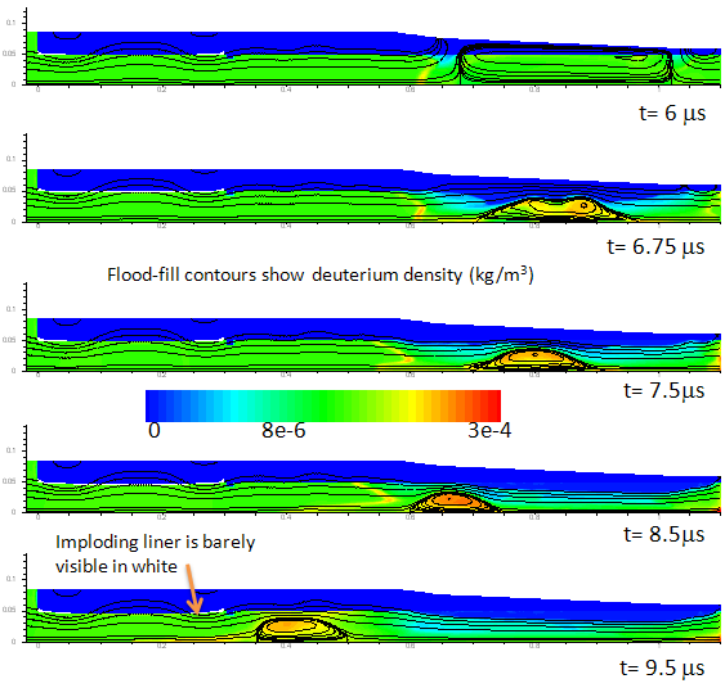

Figure 8 A typical integrated Simulation of FRC Formation and Translation Toward an Imploding Liner.

[3] All of these figures show the poloidal flux contours in black in the formation, translation and liner regions of the experiment, with dimensions in meters.

compression of the FRC. Using the designed fields as of mid-2008, we performed numerous simulations varying these parameters. Figure 9 shows the outcome of one such simulation.

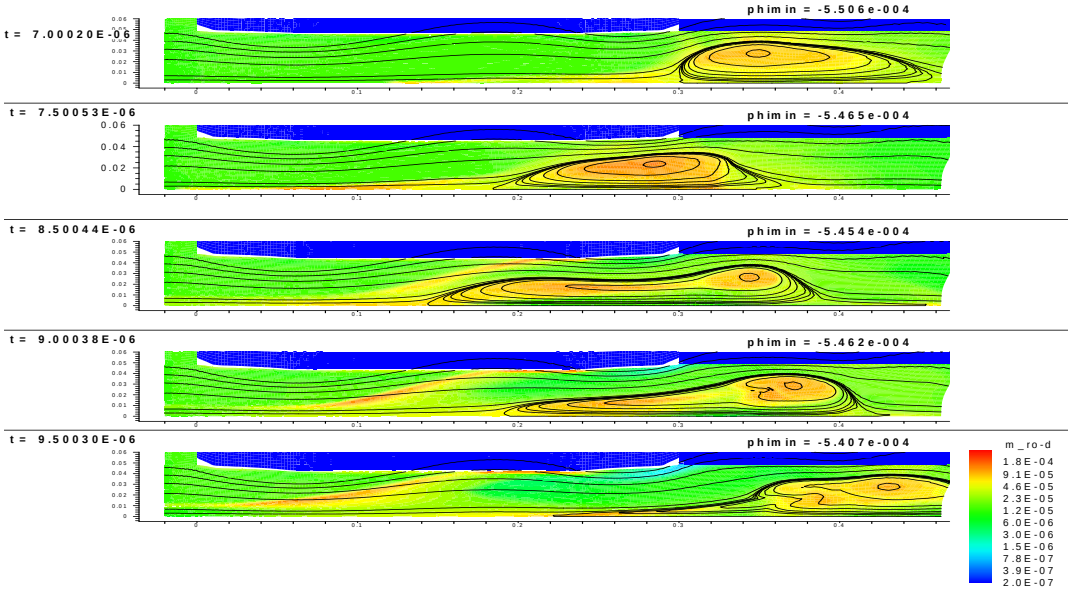

Figure 9 A Simulation where the Mirror Field is Too Large to Allow the FRC into the Liner.

In this simulation, which used a 4° formation cone angle, the mirror field is too large (even though it has not been compressed very much at 7 μs) to allow entry of the FRC into the liner. We reduced the mirror and guide fields somewhat, and obtained an opposite extreme, shown in Figure 10. Here the FRC enters the liner, but the mirror field at the entrance is unable to contain it, and the FRC bounces back out.

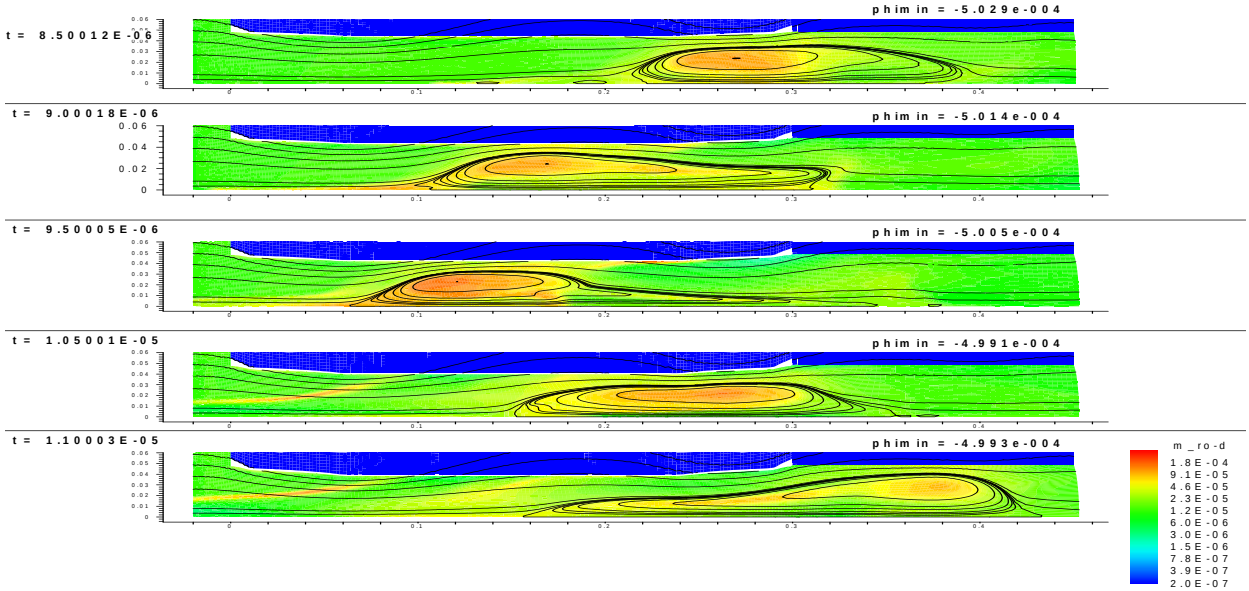

Figure 10 A Simulation where the Mirror Fields are Incapable of Containing the FRC.

By changing the cone angle to 2.5° we had a wider parameter space in which to work, and could sometimes capture part of the FRC. But it was never very reliable, and we could never capture all of it. The problem appeared to be that the field trough within the liner region was too small to hold the FRC. Working with AFRL's technologists, we recommended removing one of the mirror coils, thus widening the trough. When simulated, this design was able to capture the FRC with a variety of cone angles and timings (Figure 11). This robustness increases the likelihood of successful capture in the eventual experiments.

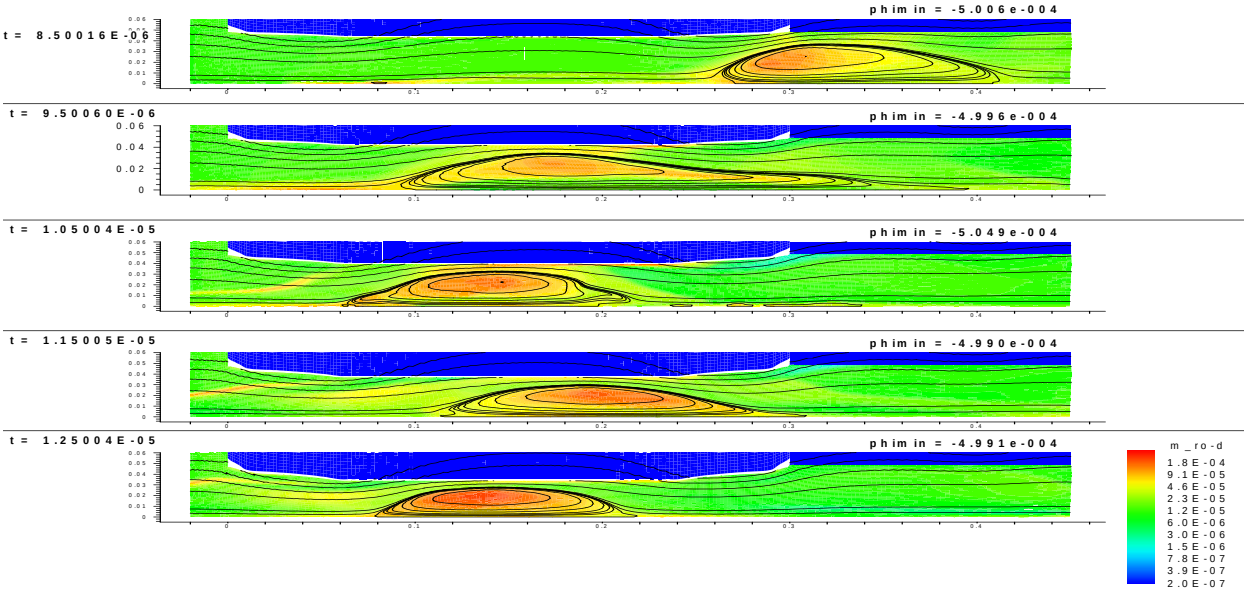

Figure 11 A Captured FRC from a 4 Degree Cone Angle Formation.

NumerEx has also employed simulation techniques to model compression of the FRC. These simulations employ quasi-lagrangian moving-grid techniques for the liner. The inner and outer radial surfaces of the liner – shown in white in the earlier figures – move with the liner until quite late in the compression phase. The remainder of the grid is numerically generated to fill the space between the axis, those surfaces, and the outer boundary

We also employ an adaptive grid for the FRC formation, translation and compression. After the FRC is captured, we reduce the size of our simulation by removing most of the formation and translation regions and continuing the compression phase. We continue to use the adaptive and ALE gridding throughout the simulation in order to improve the resolution while maintaining a reasonable timestep. The liner grid moves in a Lagrangian fashion, with the cells behind it expanding to fill the space. Interior to the liner, the grid is adapted on the gradient of the FRC's negative flux. Figure 12 shows the grid in the liner region at 14 μs, early in the compression phase.

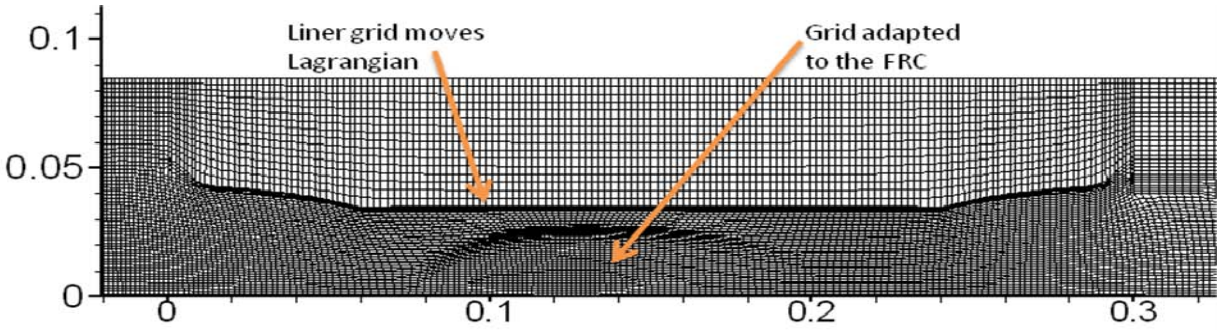

Figure 12 The liner grid moves in a Lagrangian fashion, with the cells behind it expanding to fill the space. Interior to the liner, the grid is adapted on the gradient of the FRC's negative flux.

Figure 13 shows a compression simulation in which the FRC was captured at 13.5 μs (relative to the beginning if the liner implosion). The simulation has been continued to 21.5 μs (at which point the inner radius of the liner is less than 3 mm, a compression factor of 16 relative to the liner's initial radius of 4.89 cm.

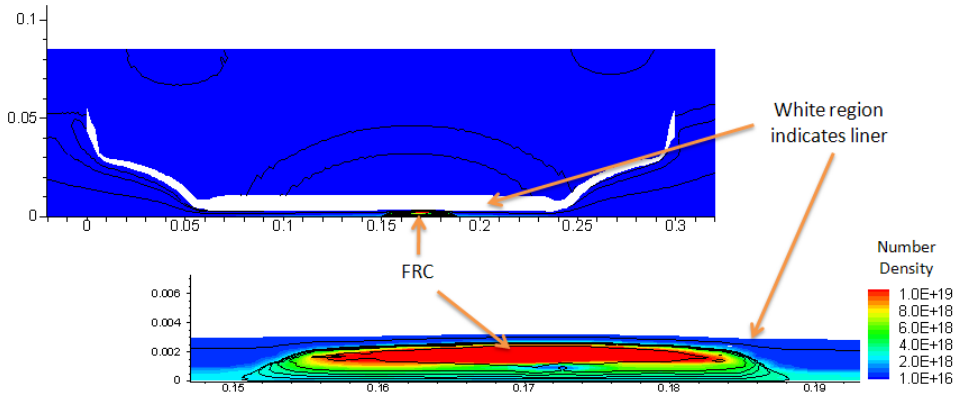

3. Figure 13 This figure from 21.5 μs shows the liner has imploded to a little under 3 mm. The liner's expansion is clearly visible as well.

3.2 Extended MHD Simulation of Formation Producing Rotation

Other physics outside the realm of MHD is relevant to FRC's. In particular, rotation has been observed to limit the experimental lifetime of FRC's, and, in the absence of applied axial electric fields, rotation is not part of the MHD physics of FRC's. However, since the Hall and thermoelectric effects of extended MHD (XMHD) can cause rotation of the FRC about the axis of symmetry, these effects need to be addressed by simulation.

We have performed XMHD simulations of FRC formation in a cylindrical configuration of the AFRL hardware. The contour plots in Figure 14 show the density and magnetic flux from one of those XMHD simulations on the right compared to a standard MHD simulation on the

left. The density and flux lines are very similar. The simulations are far from identical, however, since the standard MHD simulation shows zero azimuthal field and rotational velocity while the XMHD simulation generates a substantial amount of each, as shown in the left and right halves of Figure 15.

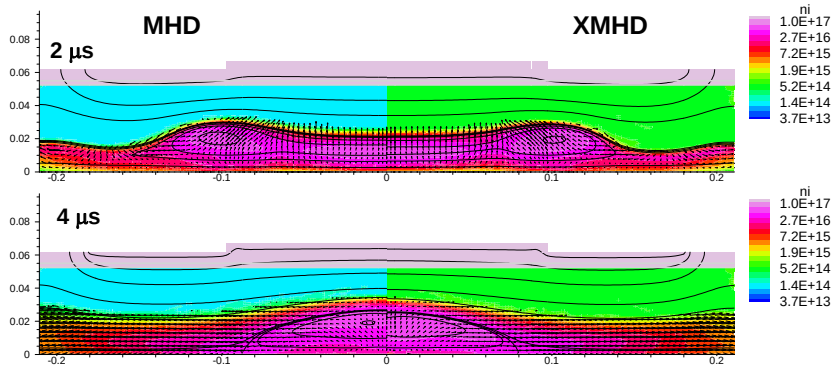

Figure 14 XMHD and MHD Simulations of Early AFRL FRC Formation Hardware using Self-Consistent Circuit Drive.

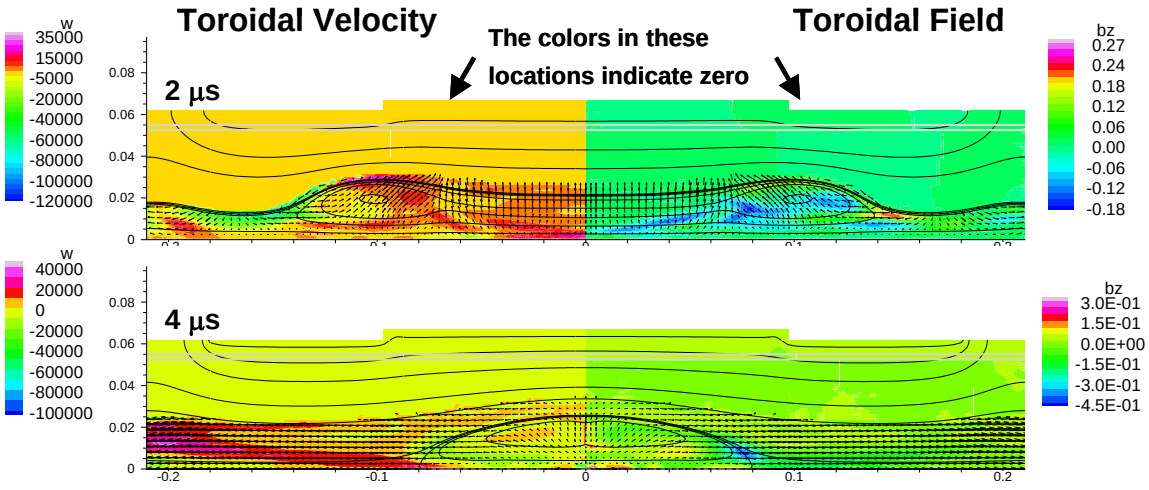

Figure 15 Rotation in an XMHD Simulation of Early AFRL FRC Formation Hardware using Self-Consistent Circuit Drive.

The rotation rate of this FRC, shown in Figure 16, rises with time, as mass is lost from the FRC. The lifetime of this simulated FRC is determined by the non-classical Chodura resistivity used. Since the Chodura resistivity model has not yet been validated for the FRC regime, the calculated FRC lifetime shown in Figure 16 is similarly uncertain. Nevertheless, it is

interesting that the rotation rate achieved here of 0.1–0.5 revolutions per microsecond is comparable to the 0.5–1.0 revolutions per microsecond observed interferometrically on FRXL at LANL, where similar fields and currents were employed.

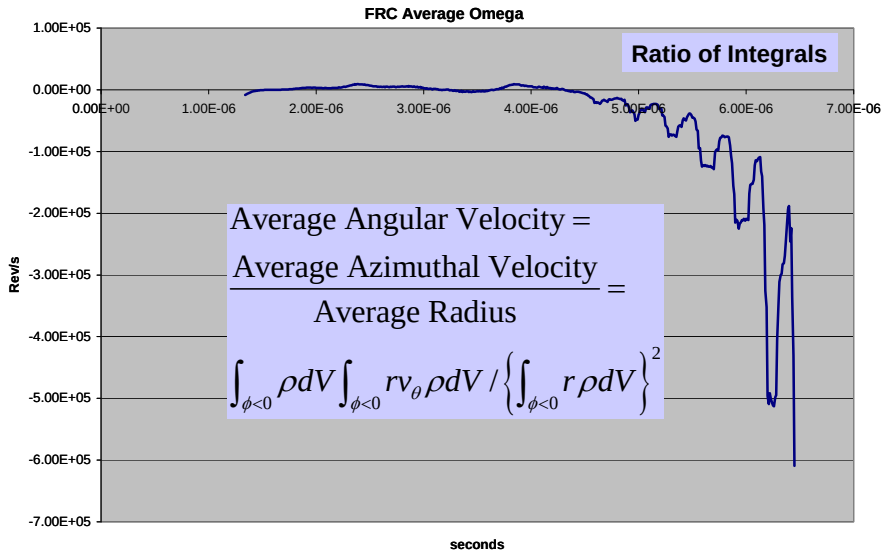

Figure 16 Average Angular Velocity from XMHD Simulation of Present AFRL FRC Formation Hardware using Self-Consistent Circuit Drive.

NumerEx co-authored a poster on this subject, Extended MHD Modeling of FRC Formation , with AFRL staff and presented it at the 20th International Conference on the Numerical Simulation of Plasmas, in October 2007.

4. Summary and Conclusions

NumerEx's has used MACH2 to simulate two different MTF concepts for pulsed neutron production. Simulations of the first concept helped in the development of a preliminary design for the generation, stagnation, and compression of ultrahigh speed plasma (UHP) flow. Simulations of the second set addressed formation, translation, capture, and compression of a field-reversed magnetized plasma configuration (FRC). Both kinds of simulations have included compression by an imploding liner driven by a fast capacitor bank.

The simulation capability evidenced here is mature enough to be used to provide direct support for experimental campaigns on either concept. This support could include shot design or analysis, and exploration of schemes for the amelioration of deleterious physical effects that might arise.

DISTRIBUTION LIST

DTIC/OCP
8725 John J. Kingman Rd, Suite 0944
Ft Belvoir, VA 22060-6218 1 cy

AFRL/VSIL
Kirtland AFB, NM 87117-5776 2 cys

Official Record Copy
AFRL/RDHP/James Degnan 1 cys

This page intentionally left blank.